

Inhibitory Contributions to Spatiotemporal Receptive-Field Structure and Direction Selectivity in Simple Cells of Cat Area 17

ADITYA MURTHY AND ALLEN L. HUMPHREY

Department of Neurobiology, University of Pittsburgh School of Medicine, Pittsburgh, Pennsylvania 15261

Murthy, Aditya and Allen L. Humphrey. Inhibitory contributions to spatiotemporal receptive-field structure and direction selectivity in simple cells of cat area 17. *J. Neurophysiol.* 81: 1212–1224, 1999. Intracortical inhibition contributes to direction selectivity in primary visual cortex, but how it acts has been unclear. We investigated this problem in simple cells of cat area 17 by taking advantage of the link between spatiotemporal (S-T) receptive-field structure and direction selectivity. Most cells in layer 4 have S-T-oriented receptive fields in which gradients of response timing across the field confer a preferred direction of motion. Linear summation of responses across the receptive field, followed by a static nonlinear amplification, has been shown previously to account for directional tuning in layer 4. We tested the hypotheses that inhibition acts by altering S-T structure or the static nonlinearity or both. Drifting and counterphasing sinewave gratings were used to measure direction selectivity and S-T structure, respectively, in 17 layer 4 simple cells before and during iontophoresis of bicuculline methiodide (BMI), a GABA_A antagonist. S-T orientation was quantified from fits to response temporal phase versus stimulus spatial phase data. Bicuculline reduced direction selectivity and S-T orientation in nearly all cells, and reductions in the two measures were well correlated ($r = 0.81$) and reversible. Using conventional linear predictions based on response phase and amplitude, we found that BMI-induced changes in S-T structure also accounted well for absolute changes in the amplitude and phase of responses to gratings drifting in the preferred and nonpreferred direction. For each cell we also calculated an exponent used to estimate the static nonlinearity. Bicuculline reduced the exponent in most cells, but the changes were not correlated with reductions in direction selectivity. We conclude that GABA_A-mediated inhibition influences directional tuning in layer 4 primarily by sculpting S-T receptive-field structure. The source of the inhibition is likely to be other simple cells with certain spatiotemporal relationships to their target. Despite reductions in the two measures, most receptive fields maintained some directional tuning and S-T orientation during BMI. This suggests that their excitatory inputs, arising from the lateral geniculate nucleus and within area 17, are sufficient to create some S-T orientation and that inhibition accentuates it. Finally, BMI also reduced direction selectivity in 8 of 10 simple cells tested in layer 6, but the reductions were not accompanied by systematic changes in S-T structure. This reflects the fact that S-T orientation, as revealed by our first-order measures of the receptive field, is weak there normally. Inhibition likely affects layer 6 cells via more complex, nonlinear interactions.

INTRODUCTION

The analysis of object motion in the visual world begins in primary visual cortex (area 17) through the action of direction-selective neurons (Hubel and Wiesel 1962). These cells re-

spond well to motion in one direction across their receptive fields and weakly or not at all to motion in the opposite direction. The mechanisms underlying this selectivity remain unresolved. However, among simple cells, important insights have been gained through the study of spatiotemporal (S-T) receptive-field structure. Many direction-selective simple cells in cat area 17 have S-T-oriented receptive fields in which response timing changes gradually across the field (Albrecht and Geisler 1991; McLean and Palmer 1989; Movshon et al. 1978; Reid et al. 1991; Saul and Humphrey 1992a). This organization confers directional tuning: a stimulus moving in a direction that successively activates receptive-field positions with progressively shorter delays, or response phases, elicits a larger net excitatory response than a stimulus moving in the opposite direction. In contrast, all nondirection-selective cells lack S-T-oriented receptive fields.

We recently showed (Humphrey and Saul 1998; Murthy et al. 1998) that S-T structure is well correlated with directional tuning in layer 4 of cat area 17. The degree to which cells are S-T oriented accounts for over half of their directional tuning on average. We also showed that a linear-nonlinear, or exponent, model (Albrecht and Geisler 1991; Heeger 1993) accounts well for directional tuning in most layer 4 cells. The model consists of two stages: a linear process in which S-T orientation confers a directional bias and a static nonlinear process that amplifies the bias to accentuate selectivity. The nonlinearity may be a threshold or, equivalently, an exponential amplification, either of which accentuates differences in response amplitude to optimal versus nonoptimal stimuli. The exponent model, however, does not account for directional tuning in layer 6 because receptive fields there are weakly S-T oriented and unrealistically large static nonlinearities are required to account for their tuning (Murthy et al. 1998). Dynamic nonlinear interactions (Emerson and Citron 1992) likely predominate in layer 6.

Intracortical inhibition is important for direction selectivity, as evidenced by the fact that blocking GABA_A-mediated inhibition reduces selectivity in most simple cells (Sillito 1984). How inhibition acts is not clear, however. One hypothesis is that it creates or enhances S-T orientation. If so, then blocking inhibition should produce a reduction in S-T orientation that is correlated with a loss of directional tuning. An alternative, though not mutually exclusive, hypothesis is that inhibition is “flat,” merely suppressing weak responses (Sato et al. 1995). It might act by lowering membrane potentials relative to spike threshold. This iceberg effect should enhance an initial directional bias but not affect response timing. In terms of the exponent model, if this was the primary inhibition, then block-

The costs of publication of this article were defrayed in part by the payment of page charges. The article must therefore be hereby marked “advertisement” in accordance with 18 U.S.C. Section 1734 solely to indicate this fact.

ing it should reduce direction selectivity and change the value of the exponent but not alter S-T orientation.

To evaluate these two hypotheses, S-T structure and direction selectivity were assessed in simple cells by measuring responses to stationary counterphasing and drifting gratings, respectively. Bicuculline methiodide (BMI), a GABA_A antagonist, was applied iontophoretically to reduce intracortical inhibition. We observed that BMI reduced direction selectivity in most cells. In layer 4, the effect was paralleled by a well-correlated reduction in S-T orientation. In layer 6, no systematic changes in S-T structure were seen. We also calculated for each layer 4 cell the value of an exponent that represents the static nonlinearity. Application of BMI reduced the exponent in most cells, but the reduction was not correlated with the changes in directional tuning. Thus inhibition affects direction selectivity in layer 4 primarily by enhancing S-T orientation and secondarily by accentuating the static nonlinearity. The measures used here do not allow us to discern how inhibition operates in layer 6.

METHODS

Physiological preparation

Details of surgical preparation are described elsewhere (Murthy et al. 1998; Saul and Humphrey 1990). Briefly, adult cats were anesthetized throughout the experiment using halothane in nitrous oxide and oxygen. A tracheostomy was performed, paralysis was induced using gallamine triethiodide and D-tubocurarine chloride, and the animal was ventilated artificially. Heart rate, mean arterial blood pressure, and the cortical electroencephalogram were monitored continuously to assess physiological state. The halothane level was adjusted to maintain the dominant frequencies of the electroencephalogram <4 Hz during all stages of the experiment. Lactated Ringer solution was infused intravenously to maintain hydration. The corneas were covered with contact lenses fitted with 3-mm artificial pupils.

Recording, visual stimulation, and iontophoresis

Extracellular recordings of single neurons were made using micropipettes filled with 0.6–2.0 M KCl (~35–20 MΩ). The recording electrode was glued to a three-barrel micropipette array, with its tip protruding from the array by ~20 μm (Havey and Caspari 1980). The array tip was broken to 5–7 μm, yielding an inner diameter of ~1.5 μm per barrel. Each barrel contained one of the following solutions: bicuculline methiodide (BMI; 2.5 mM in 165 mM NaCl, pH = 3); gamma-amino butyric acid (GABA; 0.5 M, pH = 3); or sodium acetate (2.0 M) for current balancing, to which 4% Pontamine sky blue was added. Drug barrels were subject to constant retaining currents when not in use, using –18 nA for GABA and –10 to –15 nA for BMI. Currents were controlled using a Neurophore iontophoresis unit.

Receptive fields initially were mapped manually on a tangent screen. All subsequent stimuli were presented monocularly at 57 cm on a Tektronix 608 monitor driven by a Picasso image synthesizer linked to an LSI-11/73 computer. Mean luminance was 15 cd/m² and Rayleigh-Michelson contrast was ~0.4. Simple cells were identified using standard criteria (Hubel and Wiesel 1962; Skottun et al. 1991).

Drifting sinewave gratings were used to determine each cell's optimal stimulus orientation and spatial and temporal frequency (Humphrey and Saul 1998). A set of randomly interleaved counterphasing and drifting gratings then was presented before (control) and during iontophoresis of BMI and, when possible, after recovery from the drug (postcontrol). The counterphasing grating was presented at eight spatial phases over one-half cycle of the stimulus spatial fre-

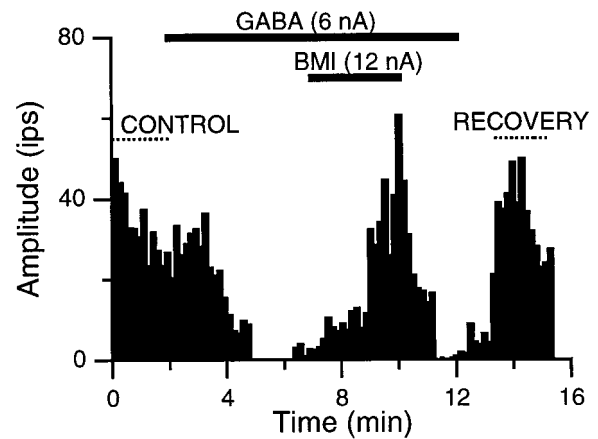


FIG. 1. Example of a titration to assess the antagonistic effects of bicuculline methiodide (BMI) on exogenously applied GABA. Plot shows 1st harmonic amplitude in response to a grating drifting in the cell's preferred direction. Horizontal bars mark the periods of drug application. Dashed line (left) marks the control response during the 1st 2 min. Iontophoresis of GABA suppressed the response within 5 min. Concurrent ejection of BMI antagonized the GABA effect and the control response returned. Cessation of BMI again led to GABA-induced suppression followed by a return to control-level responsiveness (recovery) when the GABA ejection current was turned off.

quency. Control responses usually reflected ~5 trials of each phase of the counterphase stimulus and 12–20 trials of each direction of the drifting stimulus. Trial duration was 4–6 s. The number of trials during BMI application was variable; it depended on the latency and strength of the BMI effect but was usually greater than the number of control trials.

To test the effectiveness of BMI and determine approximate levels of ejection current, we performed a standard titration procedure (Sillito 1977, 1984) on most cells. GABA was iontophored at a current that just suppressed the response to a grating moving in the preferred direction. While continuing to eject GABA, BMI ejection current was activated and increased until the response returned to control levels. One such titration is shown in Fig. 1, which plots a cell's response amplitude over time. Here, 6 nA of GABA was sufficient to suppress the control responses. Within 3 min of simultaneously applying BMI at 12 nA, the GABA effects were reversed. Cessation of both drugs led to recovery of the cell's firing rate to original values within 2 min. Having determined an effective BMI current by this procedure, we then used it as a starting value in the visual tests.

Data analysis

Action potentials were summed into peristimulus time histograms (PSTHs) to measure the average response per cycle of the periodic stimulus. First harmonic (\pm SE) amplitude and temporal phase were obtained for each PSTH, with response phase expressed in cycles relative to the stimulus (Saul and Humphrey 1990).

From responses to moving gratings we computed a *directional index* (DI) as $DI = (PD - NPD)/(PD + NPD)$, where PD and NPD are the response amplitudes in the preferred and nonpreferred directions of motion, respectively. Ratios of 0 and 1, respectively, reflect no and complete direction selectivity. An estimate of the standard error of DI was obtained from separate DI measurements on individual sets of trials. Only cells with DIs >0.33 were considered selective and subsequently tested with BMI.

Responses to counterphasing gratings were used to characterize S-T receptive-field structure. We relied primarily on a recently developed method described in detail by Murthy et al. (1998). Because the present results require understanding the method and its rationale, we summarize it here. In a strictly linear model of directional tuning, a stationary, counterphasing sinewave grating elicits predictable pat-

terns of response amplitude and phase as a function of grating position in the simple-cell receptive field. For a completely direction-selective cell, as the spatial phase of the grating changes, response phase changes monotonically with a slope of 1.

In contrast, amplitude remains constant and an amplitude modulation (AM) ratio, defined as $[1 - (\text{min amp}/\text{max amp})]$, is 0. For a directionally nonselective cell, response phase is constant (i.e., slope = 0) within each half of the grating cycle. However, amplitude varies sinusoidally with spatial phase and the AM ratio is 1. For a cell with intermediate directional tuning, amplitude also fluctuates sinusoidally and the modulation ratio lies between 0 and 1, and the response phase versus spatial phase data do not follow a straight line but are fit by an arctangent function (e.g., Fig. 4A). We used this fit to derive a *spatiotemporal index* (STI) for each cell that reflects the slope of the function at the spatial phase generating the maximum response. The STI is a metric that summarizes the S-T orientation of the receptive field. STI is 1 and 0, respectively, for receptive fields that are completely S-T oriented or unoriented. In a strictly linear system, S-T orientation determines directional tuning; thus STI and DI values are equal (see Murthy et al. 1998 for derivation of the relationship).

In a linear system, S-T orientation and AM to counterphased gratings are related inversely. Hence either or both measures potentially predict direction selectivity. However, cells are subject to nonlinearities that, in the context of direction selectivity, have been modeled as static nonlinearities (Albrecht and Geisler 1991; Heeger 1993). They accentuate differences in amplitude to optimal versus nonoptimal stimuli and hence increase AM ratios beyond those due to linear summation. Thus conventional linear predictions of direction selectivity that use response amplitude (e.g., Reid et al. 1991) underestimate the linear contribution because of nonlinear amplitude distortion. In contrast, response phase is not affected by static nonlinearities, so the phase-based measure, STI, provides a better estimate of the linear contribution. We used the STI to quantify changes in the temporal organization of the receptive field induced during blockade of GABA_A-mediated inhibition and to estimate their linear contribution to changes in direction selectivity. As described in the RESULTS, we also employed the STI to evaluate the contribution of static nonlinear processes to directional tuning.

In addition to the STI, we used phase and amplitude measures to make conventional linear predictions of directional tuning for comparison with our STI-based measures and to examine relationships between S-T structure and direction selectivity that require information about amplitude. We used a superposition method similar to that of Jagadeesh et al. (1997). It derives from the fact that the sum of two counterphasing gratings in spatial and temporal quadrature constitutes a drifting grating. Assuming linearity, the responses to the counterphasing gratings equal those to the drifting grating. We identified pairs of gratings in spatial quadrature from the eight spatial phases tested. First harmonic response amplitude and phase at each spatial phase were expressed as a vector in polar coordinates. Temporal quadrature was simulated by translating the response phase of one grating in each pair by a quarter cycle. The paired responses were summed vectorially to give predicted responses to a grating drifting in each of two directions. A mean predicted amplitude and phase¹ was calculated from the four quadrature pairs. Predicted amplitudes to each direction of motion also were used to derive a predicted DI.

For ease in viewing, the counterphase data from control trials were normalized in three ways. First, response phase was plotted so as to increase with increasing spatial phase, thereby normalizing for preferred direction of motion. Second, the response amplitude and phase functions were shifted equally horizontally so that amplitude peaked

near 0.25 and 0.75 cycles. Third, the phase functions were shifted vertically to pass through the origin. The BMI and postcontrol data were shifted similarly to maintain spatial phase correspondence in the different conditions.

Reconstructing recording sites

Electrode penetrations were marked by extracellular deposits of Pontamine dye. Animals were administered a lethal dose of Nembutal and perfused with aldehydes. Brain sections were stained for Nissl substance, electrode tracks were reconstructed (Murthy et al. 1998), and cells' recording locations were assigned using the laminar criteria of O'Leary (1941; Humphrey et al. 1985).

Statistics

All comparisons of means were made using a paired *t*-test (Miller and Freund 1985). Pearson product-moment (*r*) or Spearman rank (*r_s*) correlations were used for other comparisons.

RESULTS

Results are based on 27 simple cells from 17 cats; 17 cells were in layer 4 and 10 were in layer 6. We first describe changes in direction selectivity and S-T receptive-field structure produced by GABA_A blockade in three representative cells. We next summarize how the blockade affected the population and show that effects on S-T structure differed between layers 4 and 6. We then show that inhibition contributes to direction selectivity in layer 4 mainly by increasing S-T orientation.

Effect of BMI on direction selectivity and S-T structure in individual cells

Figure 2A shows average responses of a layer 4 cell to one cycle of a sinewave grating drifting at 2 Hz during control, BMI, and postcontrol conditions. During control trials, the cell was highly direction selective (DI = 0.92), discharging vigorously in the preferred direction of motion (Fig. 2A, *bottom*) and weakly in the nonpreferred direction (*top*). Within 4 min of iontophoresing BMI, selectivity was abolished (DI = 0). To facilitate comparison, control responses (•••) are superimposed on the BMI data. Interestingly, the loss of direction selectivity in this cell reflected both an increase in response amplitude to the nonpreferred direction and a decrease in amplitude to the preferred direction. Additionally, there were shifts in response timing that were most visible in the preferred direction: the response during BMI was delayed by about a quarter cycle relative to the control response. The drug effect was reversible as evident in the postcontrol trials taken within 3 min of terminating BMI. We show later that BMI-induced changes in amplitude and timing to moving gratings reflect changes in the amplitude and timing structure of the receptive field.

The cell's S-T structure during the three conditions is shown in Fig. 3. The PSTHs illustrate responses to a 2-Hz counterphasing grating presented at different spatial phases in the receptive field. During control trials (Fig. 3A), the receptive field displayed clear S-T orientation, as evidenced by a gradual shift in response timing with increasing spatial phase. To further illustrate this, mean phase values are plotted against spatial phase in Fig. 4A. An arctangent function fit to the

¹ Response phases also were normalized to compensate for the difference between the spatial phases of the quadrature pairs. Taking spatial phases of 0 and 0.25 as the first or reference pair, we subtracted 0.0625 cycles from the second quadrature pair to simulate spatial alignment. Similarly, 0.125 and 0.1875 cycles were subtracted from the third and fourth pairs, respectively.

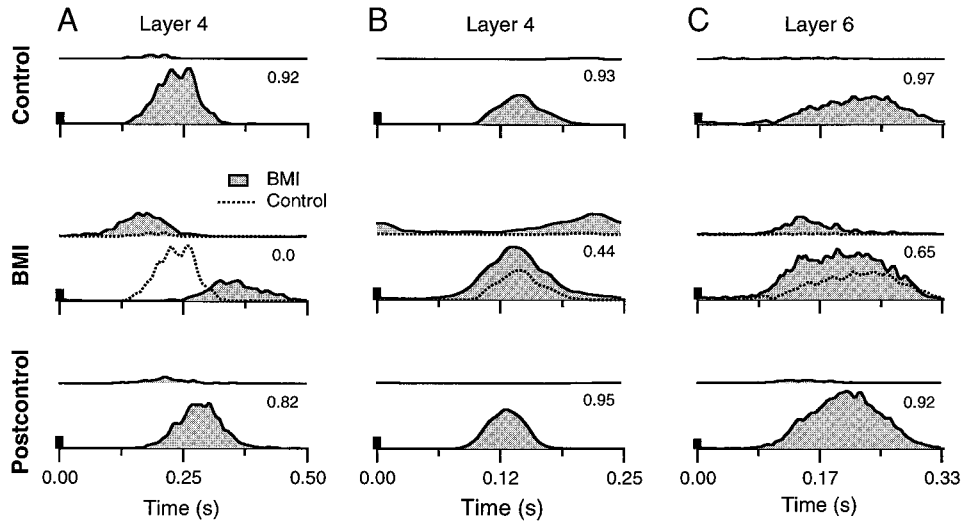


FIG. 2. Responses of 3 cells (A–C) to drifting gratings during control, BMI, and postcontrol conditions. For each condition, each pair of peristimulus time histograms (PSTHs) shows average discharge profiles to 1 cycle of the grating moving in the preferred (bottom) and nonpreferred (top) direction. For the BMI conditions, superimposed control responses (•) help to illustrate the drug-induced changes in amplitude and/or timing. Directional index (DI) values are indicated (right) in each pair of PSTHs. For responses in A–C, the grating drifted at 2, 4, and 3 Hz, respectively; firing rate scaling (vertical bars) is 50, 22, and 26 impulses (ips), respectively. See text for details.

response phase data yielded an S-T orientation index (STI) of 0.62.

Figure 3B illustrates the changes in S-T structure during iontophoresis of BMI. Control responses are shown superimposed on the corresponding BMI profiles. Each pair of PSTHs is normalized to equate maximum firing rates to better illustrate the relative changes in timing induced by the drug. Reduction of inhibition produced clear timing changes at all spatial phases; responses were elicited later than in control trials. These shifts are defined as phase lags. In Fig. 4C the lags are plotted

as increases in response phase, and all were statistically significant ($P < 0.05$).

Figures 3B and 4C also reveal that the BMI-associated response did not lag the control discharge uniformly across spatial phase. Phase lags were greatest at zero spatial phase and progressively less up to ~ 0.44 cycles. Because of symmetry (Movshon et al. 1978; Reid et al. 1991), the same timings were duplicated in the second half cycle. The changes resulted in much more uniform timing within each half of the grating cycle, and the receptive field became essentially S-T unori-

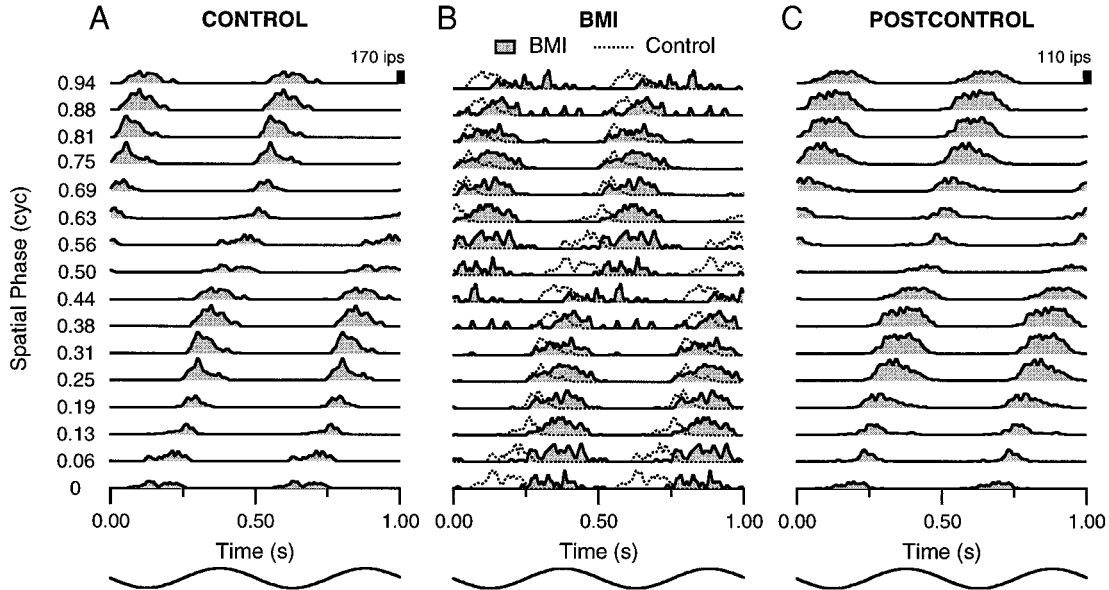


FIG. 3. Responses of the cell in Fig. 2A to a stationary grating undergoing sinusoidal luminance modulation at 2 Hz. Two cycles of stimulation are shown, with the second response in each PSTH being a duplicate of the first. A: control responses at 16 spatial phases spanning a grating cycle. First half-cycle was tested; symmetry allowed responses to be duplicated to complete the second half-cycle. Receptive field was spatiotemporally (S-T) oriented. B: responses during application of BMI. To clarify the changes in response timing, BMI (—) and control (---) responses are superimposed, and each pair of histograms is normalized to equate maximum firing rates. BMI produced clear changes in timing at all spatial phases, resulting in a loss of S-T orientation. C: postcontrol responses show the reestablishment of S-T orientation.

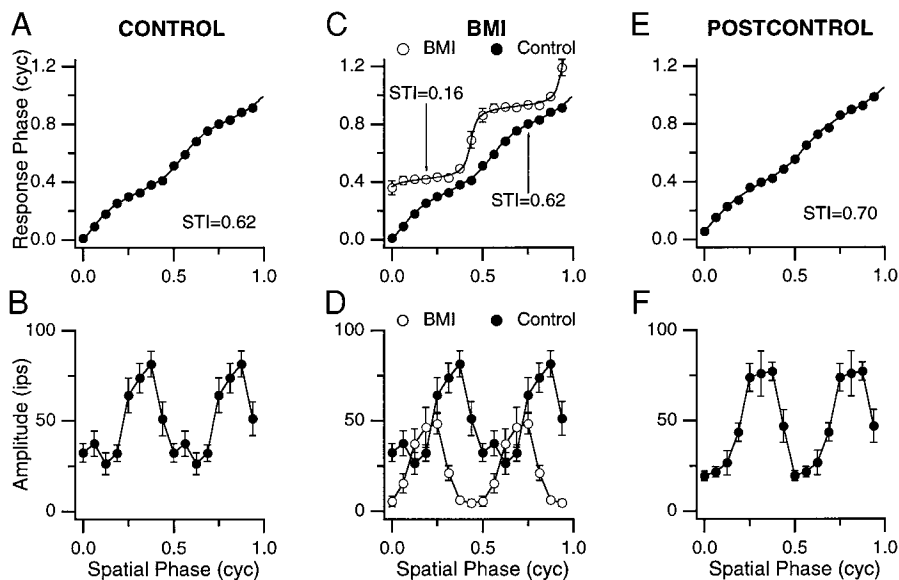


FIG. 4. A and B: response phase and amplitude plotted as a function of stimulus spatial phase for the control responses in Fig. 3A. Response phase increased monotonically with spatial phase. An arctangent fit to the phase data (— in A) yielded a spatio-temporal index (STI) of 0.62. C and D: responses during iontophoresis of BMI (○); control responses (●) are shown for comparison. Response phase at all positions was significantly delayed by BMI, compared with controls, and the STI was reduced to 0.16. Like response phase, amplitude changed systematically, and the amplitude ratio increased from 0.67 to 0.90. E and F: during the postcontrol run, S-T orientation and response amplitude and its modulation returned to approximate control values. All error bars in this and the following figures indicate ± 1 SE.

ented (STI = 0.16). The loss of S-T orientation would be expected in a linear model of directional tuning.

In such a model, amplitude profiles vary systematically with direction selectivity (see METHODS) (Murthy et al. 1998). For a cell with a DI of 1.0, amplitude should be constant (i.e., unmodulated) as the position of a counterphased grating changes. As DI decreases, the degree of modulation should increase. Figure 4D shows that BMI altered the AM ratio, increasing it to 0.90 from a control value of 0.67. Overall, then, the changes in phase and amplitude during GABA_A blockade are consistent with a linear spatiotemporal model of direction selectivity. This was supported by the conventional linear predictions using the superposition method: BMI reduced predicted DI from 0.47 to 0.08.

After cessation of the GABA_A antagonist, the control pattern of response timings was reinstated (Figs. 3C and 4E), S-T orientation was again clearly discernable (STI = 0.70), and the AM ratio decreased to 0.75, its approximate control value. The conventional linear prediction of direction selectivity (0.40) also returned to a near-control value.

The aforementioned cell was one of the most striking examples of the effects of reducing inhibition. Another simple cell in layer 4, the direction selectivity of which was reduced but not abolished by BMI, is shown in Fig. 2B. This result was the more typical one. The cell was highly direction selective (DI = 0.93) during control trials. Within 2 min of applying BMI, responses to both directions of motion increased by about the same amount. However, the relative increase in response to the nonpreferred direction was greater, resulting in a 53% reduction in DI. The effect of BMI was reversible, as seen in the postcontrol data. Unlike the previous cell, these changes were not accompanied by any significant shift in response phase to the drifting grating.

Figure 5, B and C, shows that the BMI-induced changes in the cell's direction selectivity reflected changes in S-T orientation: STI decreased from 0.51 to 0.18. Unlike the previous cell, timing changes were associated with phase leads not lags, and they did not occur at all positions. Significant shifts occurred only between spatial phases of 0.25 and 0.38 cycles (and

0.75–0.88 cycles). However, as before, the phase shifts resulted in more uniform timing across the receptive field.

The decrease in this cell's direction selectivity also was accompanied by increases in response amplitude to the counterphasing grating (Fig. 5D), although the AM ratio changed little, from 0.89 to 0.81. The superposition analysis predicted a reduction in DI from 0.31 to 0.19. After cessation of the GABA_A block, timings, S-T orientation and amplitudes returned to approximate control values (not illustrated).

Figure 2C illustrates the effect of reducing inhibition on a simple cell in layer 6. Like the previous example, the response to each direction of motion increased during BMI but the relative change in the nonpreferred direction was greater, reducing DI from 0.97 to 0.65. Strong directional tuning returned in the postcontrol trials. Figure 6 illustrates the cell's S-T structure. Unlike the layer 4 cells, this receptive field lacked prominent S-T orientation during control trials (STI = 0.14; Fig. 6, A and C). BMI induced slight phase leads at some positions but the timing shifts did not significantly change S-T orientation (Fig. 6, B and C). This is not surprising given the initially low S-T orientation. The reduction in DI was accompanied by an increase in the AM ratio, from about 0.67 to 0.81 (Fig. 6D). The superposition analysis predicted a reduction in DI from 0.37 to 0.17. Thus for this and two other layer 6 cells (not illustrated), changes in S-T structure correctly predicted the reduction in direction selectivity. However, unlike layer 4 cells, the changes largely reflected alterations in the AM ratio rather than in S-T orientation. Further, in other layer 6 cells (see following text) the minor changes in S-T structure induced by GABA_A blockade predicted an increase in DI but a decrease was seen. Overall, changes in S-T structure accounted poorly for changes in directional tuning in this and other layer 6 cells.

Population results

EFFECT OF BMI ON DIRECTION SELECTIVITY. Figure 7 plots the DI under control versus BMI conditions for each cell. Most (89%) cells lie significantly below the line of unity slope, indicating that the drug reduced their direction selectivity. However, the strength of the effect varied widely, from slight

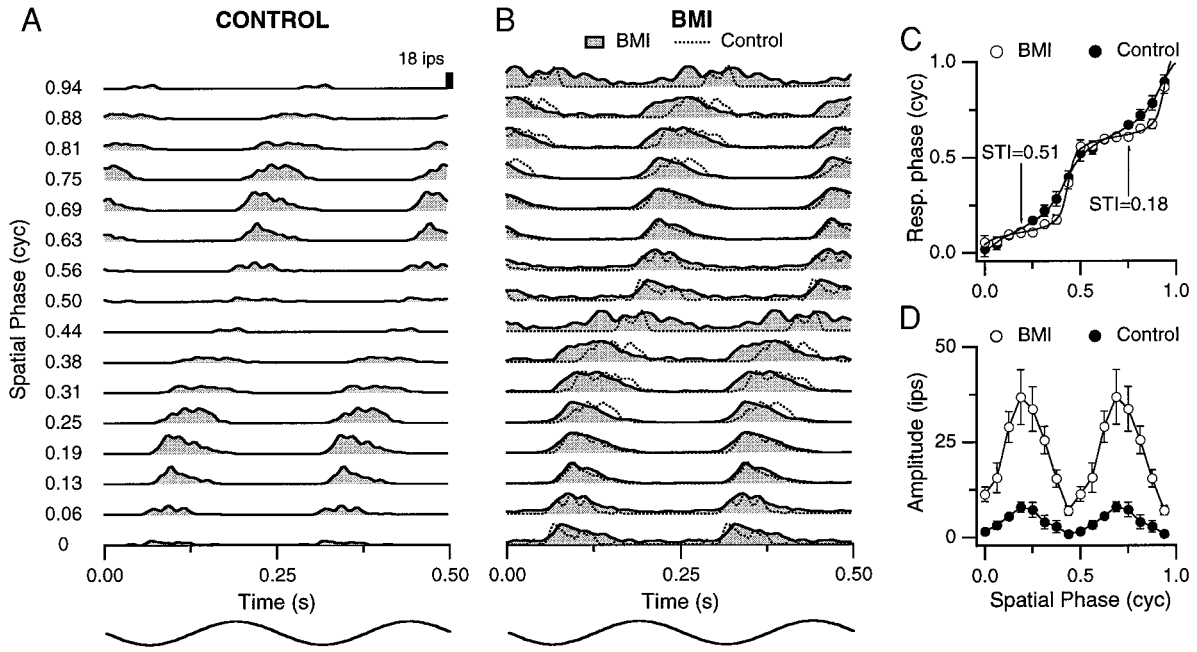


FIG. 5. Effect of BMI on responses of the cell in Fig. 2B to a grating counterphasing at 4 Hz. Conventions are as in Figs. 3 and 4. *A*: receptive field was moderately S-T oriented during control trials. *B*: BMI produced a leftward shift (i.e., phase lead) in response timing at spatial phases 0.25–0.38 cycles (and 0.75–0.88 cycles). *C*: response phase vs. spatial phase for control and BMI conditions. BMI application reduced S-T orientation. *D*: response amplitude versus spatial phase for the 2 conditions shows that BMI increased amplitude.

reductions to complete loss. For 37% of the cells, DI was reduced to <0.33 , our criterion for selectivity, but most of these cells maintained a directional bias. Interestingly, two cells reversed their preferred direction: one was patently selective and the other was biased for direction.

There was no laminar difference in the effect of BMI on

direction selectivity. Mean control DI was $0.80 \pm \sim 0.05$ both for layers 4 and 6. During BMI application the absolute value of each mean dropped to 0.41 ± 0.06 and 0.51 ± 0.06 , respectively. Both values were significantly lower than normal ($P < 0.05$) but not different from each other ($P > 0.1$).

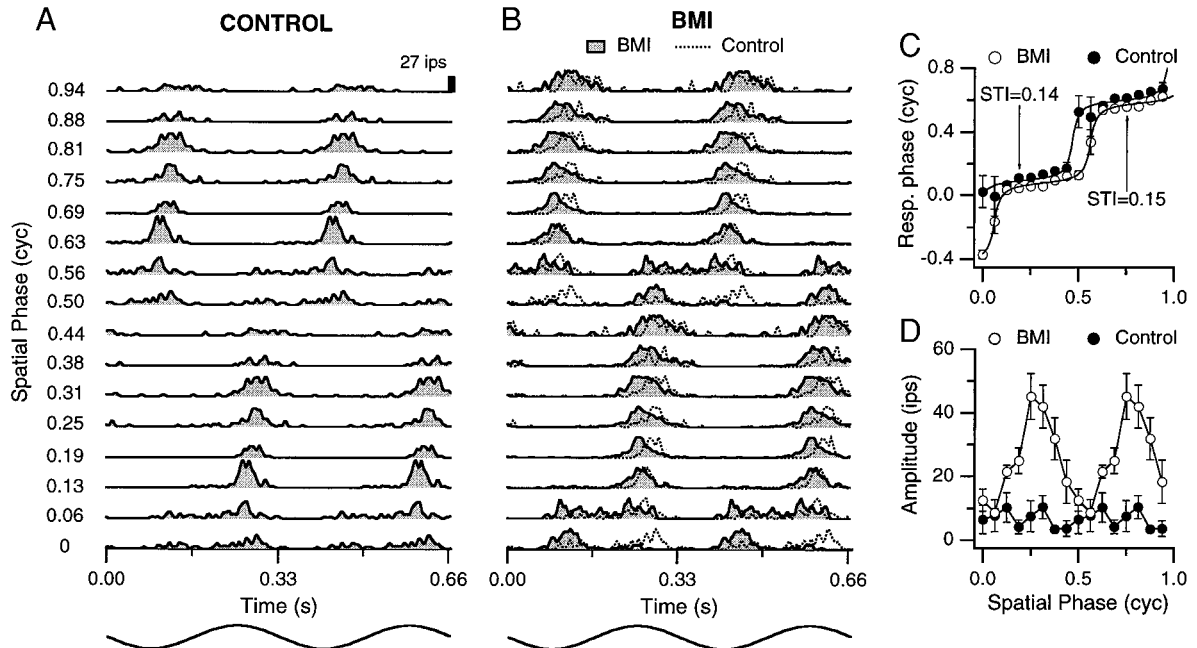


FIG. 6. Effect of BMI on responses of the layer 6 cell in Fig. 2C to a grating counterphasing at 3 Hz. *A*: this direction-selective receptive field was weakly S-T oriented in control trials. *B*: BMI produced slight phase leads at most spatial phases, relative to control responses. *C*: response phase vs. spatial phase data reveal no significant change in S-T orientation induced by BMI. *D*: BMI increased response amplitude at most spatial phases. Conventions are as in Figs. 3 and 4.

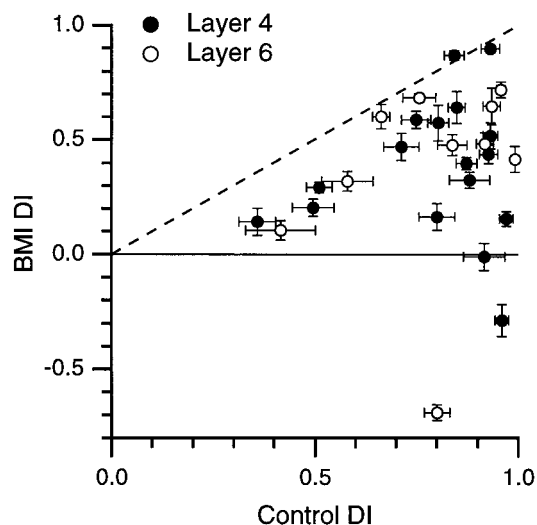


FIG. 7. Comparison of the directional indexes of single cells during control and BMI conditions. BMI reduced direction selectivity in most cells, but the effect varied widely across the sample. Two cells below the zero line reversed their preferred direction of motion during drug application.

EFFECT OF BMI ON SPATIOTEMPORAL STRUCTURE. Clear differences between layers 4 and 6 were observed in the action of BMI on S-T structure. Figure 8A plots the S-T orientation of each cell during control and BMI conditions. During control trials, layer 4 cells displayed a wide range of STI values, from 0.16 to 0.83 (mean = 0.41 ± 0.04). During blockade of inhibition, STI was significantly reduced in 12 of the 16 cells (mean STI = 0.17 ± 0.03 ; $P < 0.05$). Similar to the effect on DI, however, the change in STI varied among cells; a few became completely S-T unoriented but most continued to display an obvious spatiotemporal bias.

As noted above, direction-selective cells in layer 6 normally exhibit little or no S-T orientation. In the present sample, control STIs ranged from 0 to 0.22 (mean = 0.09 ± 0.02). Reducing GABA_A-mediated inhibition did not systematically affect STI in this layer (mean STI = 0.13 ± 0.03). It was unaltered in three cells, increased slightly in four cells, and reversed slightly in one cell.

Figure 8B summarizes the effect of BMI on predicted direction selectivity, obtained using the superposition method. Although inclusion of amplitude in these conventional predictions changed the distributions relative to Fig. 8A, similar trends were observed. In layer 4, BMI caused changes in S-T structure in most (81%) cells that predicted a reduction in DI, from 0.33 ± 0.04 to 0.21 ± 0.04 ($P < 0.05$), on average. In layer 6, predicted DI was not consistently affected (control mean = 0.14 ± 0.04 ; BMI mean = 0.18 ± 0.04). Because the action of BMI on S-T structure was clearest in layer 4, we focus on this layer for the rest of the RESULTS.

JOINT EFFECT OF BMI ON S-T STRUCTURE AND DIRECTION SELECTIVITY IN LAYER 4. Figure 9 shows that the changes in direction selectivity during blockade of GABA_A mediated inhibition largely were accounted for by the alterations in S-T receptive-field structure. Figure 9A plots the percent change in STI versus percent change in DI induced by BMI. Most cells lie in the third quadrant, confirming that a reduced DI was almost always accompanied by a lowered STI. For these cells, reductions in the two measures were well correlated ($r = 0.81$).

A similar analysis comparing conventional linear predictions against actual direction selectivity is shown in Fig. 9B. The change in DI was correlated moderately with the change in predicted DI, although the relationship was more variable ($r = 0.67$) than between DI and STI.

We previously showed that the S-T structure of most layer 4 receptive fields accounts for a substantial fraction of their directional tuning (Murthy et al. 1998), although linear predictions nearly always underestimate actual tuning (Albrecht and Geisler 1991; DeAngelis et al. 1993b; Reid et al. 1991). Here we asked whether S-T structure accounted for a similar fraction of direction selectivity in control and BMI conditions despite the drug-induced changes. Figure 9C plots the proportion of DI attributable to STI for each cell in the two conditions. Values for 9 of the 16 cells fell on or near the line of unity slope, indicating that S-T orientation contributed to a similar proportion of directional tuning in both conditions. For four additional cells (with ordinate values of 0) STI accounted for a moderate to high proportion of DI in control trials. During BMI, their STIs dropped to near zero (mean = 0.04), as did most of their DIs (mean = 0.16), again revealing a strong dependence of directional

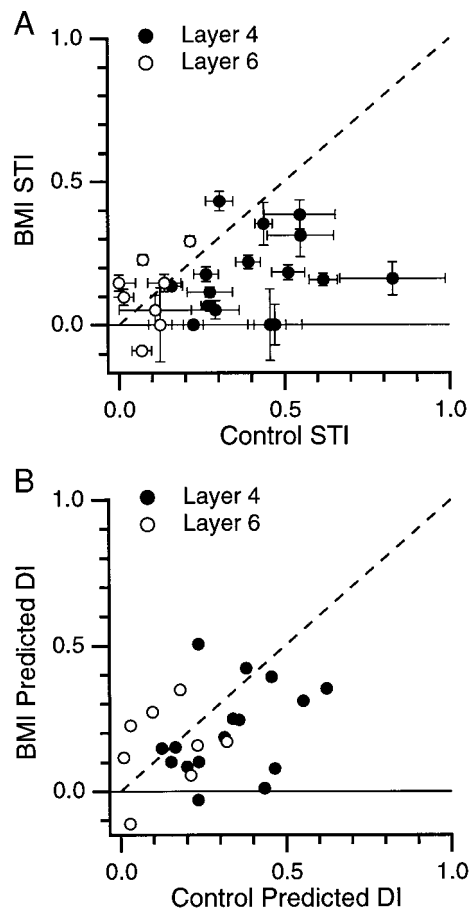


FIG. 8. A: comparison of S-T orientation indexes during control and BMI conditions. Most layer 4 cells (\bullet ; $n = 16$) lie below the line of unity slope, revealing that BMI reduced their STIs. In contrast, the effect of BMI on STI in layer 6 cells (\circ ; $n = 8$) was weak and variable, with no net change across the sample. B: conventional linear predictions of direction selectivity for the same cells during control and BMI conditions reveals similar trends. Three cells were omitted from both scatterplots due to unreliable counterphase responses during 1 condition.

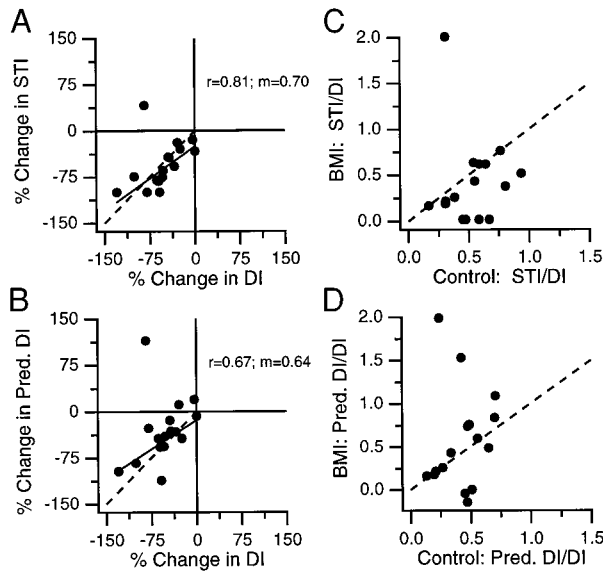


FIG. 9. Relationship between BMI-induced changes in DI and S-T receptive-field structure for layer 4 cells. *A* and *B*: plots of the percent change in DI vs. percent change in STI and predicted DI, respectively, induced by BMI. For most cells, the reduction in DI was accompanied by a proportional reduction in STI and predicted DI. One cell reversed preferred direction during BMI and is represented as a -130% change in DI. For another cell, linear predictions incorrectly indicated a slight reversal in preferred direction, which is represented in *B* as -110% . Correlation coefficient and slope are indicated by r and m , respectively. *C* and *D*: plots of the fraction of DI accounted for by STI and predicted DI, respectively, in control and BMI conditions. See text for description.

tuning on S-T orientation. For the three other cells, the fraction differed significantly in the two conditions. A similar analysis, done using conventional linear predictions, is shown in Fig. 9*D*. Again, the fraction of selectivity ac-

counted for by the predictions was roughly similar in the two conditions for about three-fourths of the cells.

Taken together, these results indicate that GABA_A-mediated inhibition affects directional tuning in layer 4 largely through changes in spatiotemporal receptive-field structure, particularly by increasing S-T orientation.

EFFECT OF BMI ON RESPONSE AMPLITUDE TO DRIFTING GRATINGS. Because the BMI effects on direction selectivity in layer 4 largely could be accounted for by changes in S-T structure, we wondered whether alterations in response amplitude to drifting gratings could be predicted similarly from the counterphase data. Using the superposition method, we computed a predicted response amplitude for each direction of motion in the control and BMI conditions. Subtraction of the BMI predicted amplitudes from control predicted amplitudes yielded the predicted amplitude change for each direction due to the reduced inhibition. Likewise, the measured amplitudes to drifting gratings in the two conditions were subtracted to yield the observed amplitude change due to BMI.

Figure 10, *A* and *B*, plots the predicted versus observed amplitude change for the preferred and nonpreferred directions of motion, respectively. For most cells, BMI increased response amplitudes to drifting gratings for each direction. For both directions, most points in the sample fell on or near the line of unity slope, indicating that the amplitude changes were well accounted for by the predictions. Interestingly, BMI caused a decrease in amplitude in three cells (Figs. 2*A* and 10*A*), which were predicted by the changes in S-T structure. In general, BMI had a similar effect on response amplitudes in individual cells to drifting and counterphasing gratings, increasing amplitudes to both stimuli in most cells, and decreasing it to both in the three cells. The stronger responses during BMI were expected given its action in reducing inhibition. The

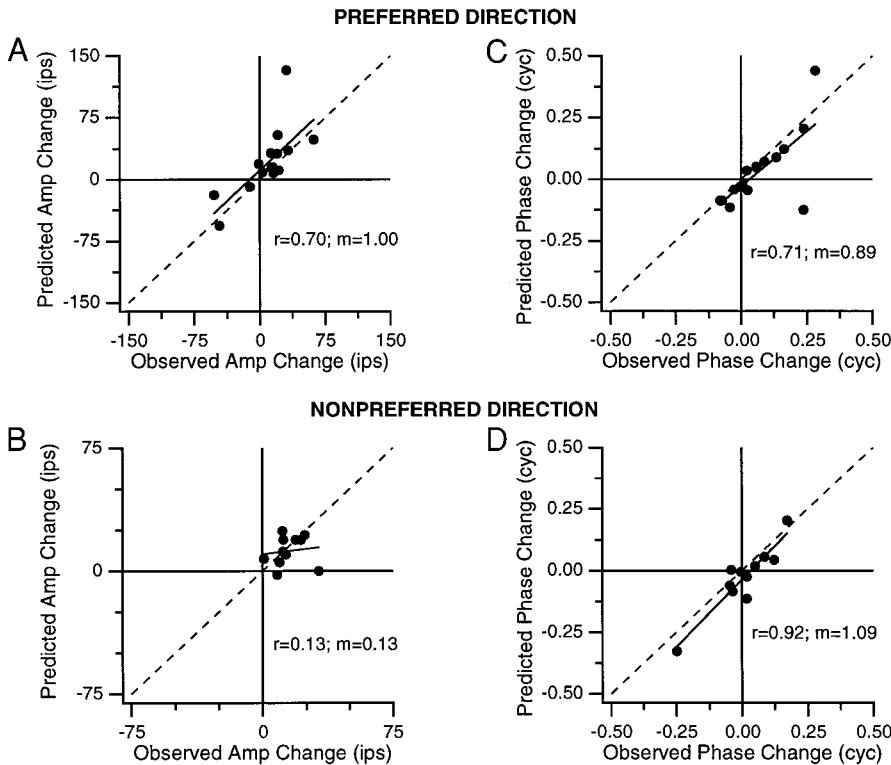


FIG. 10. Relationship between the BMI-induced changes in response amplitude and phase to drifting gratings and that predicted from changes in S-T structure. *A* and *B*: change in amplitude—either an increase or decrease in mean firing rate—for the preferred direction, was well accounted for by the linear predictions. A weaker relationship held for the nonpreferred direction. *C* and *D*: change in response phase—either a phase lead (negative cycle) or lag (positive cycle)—to each direction was well accounted for by the linear predictions. Four cells for which control amplitudes were <2 ips are omitted from *B* and *D*.

weaker responses in a few cells were surprising, and may reflect the action of BMI on complex neural networks (e.g., disinhibition of inhibitory neurons feeding back on the cell being studied).

EFFECT OF BMI ON TIMING OF RESPONSE TO DRIFTING GRATINGS. The reduction in direction selectivity often was accompanied by a shift in the phase of response to the drifting grating (e.g., Fig. 2A). To assess whether these timing shifts also could be explained by changes in S-T structure, we performed the superposition analysis as above but focused on response phase. Figure 10, C and D, plots the change in predicted versus observed phase for the preferred and nonpreferred direction, respectively. For most layer 4 cells, BMI induced a response phase lag to drifting gratings; other cells underwent a slight phase lead. Importantly, most of these shifts were well predicted by the concomitant changes in S-T structure.

Although the BMI-induced changes in timings and amplitudes across the receptive field underlie the shifts in timing to moving stimuli, the causal relationships are not obvious from simple inspection of the static plots. Clearly, the response to a drifting grating reflects the convolution of the stimulus profile with the amplitude and temporal structure of the receptive field. For layer 4 simple cells, the superposition method captures essential aspects of these S-T interactions, revealing causal relationships between changes in S-T structure and changes to moving gratings.

DOES BMI ALSO AFFECT DIRECTION SELECTIVITY IN LAYER 4 VIA CHANGES IN THE STATIC NONLINEARITY? Although S-T structure correlated with DI in control and BMI conditions, linear predictions underestimated DI in most cells, indicating that nonlinear processes also operate in both conditions. In layer 4 these processes can be modeled as a static nonlinearity—an exponent—that follows linear summation (Albrecht and Geisler 1991; Heeger 1993; Murthy et al. 1998). Here we asked whether reduction of inhibition altered the exponent and, if so, whether the change contributed systematically to decreased directional tuning.

The nonlinearity was evaluated using a procedure developed by Murthy et al. (1998). To summarize, the exponent can be estimated using the amplitude and STI data. One compares the modulation in amplitude to a counterphased grating with the modulation expected from the STI value. As described in METHODS, the STI fully predicts the AM ratio and the two measures are inversely related if summation is strictly linear. If, however, a static nonlinearity follows the linear stage, then the modulation predicted by the STI will underestimate the actual modulation. This is because the nonlinearity accentuates differences in amplitude to the null and optimal spatial phases of the grating, increasing modulation. The nonlinearity can be estimated by calculating an exponent, n_{CG} , which is required to raise the STI-predicted AM ratio to that observed. We previously showed (Murthy et al. 1998) that n_{CG} approximates another exponent, n_{DG} , that is required to precisely match linearly predicted and actual direction selectivity to drifting gratings. Thus n_{CG} is a reasonable estimate of the static nonlinearity. Here we compared n_{CG} in control and BMI conditions for each layer 4 cell.

Figure 11A shows that BMI application reduced the value of n_{CG} in most cells; geometric means were 1.7 and 1.1 in control

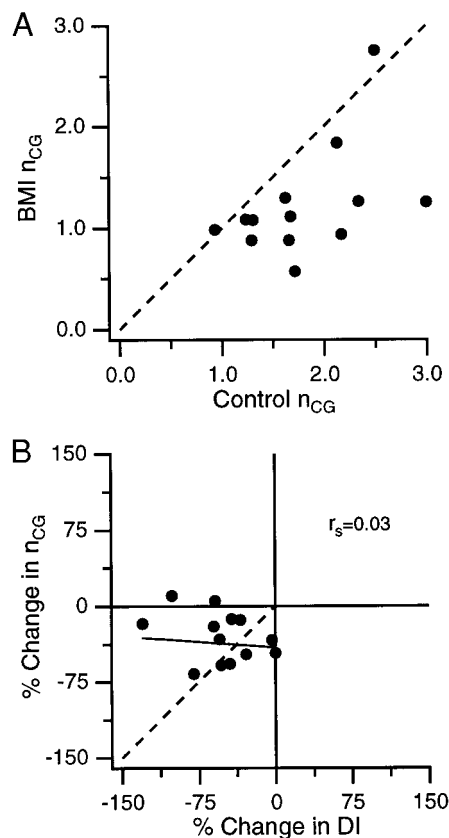


FIG. 11. Effect of BMI on the static nonlinearity, n_{CG} , and its relationship to directional tuning. A: plot of n_{CG} values in control vs. BMI conditions for 13 cells in which the exponent could be reliably estimated. BMI reduced the exponent in nearly all cells. B: plot of the percent changes in n_{CG} vs. DI induced by BMI. Reductions in the 2 measures were not correlated. r_s , Spearman rank correlation coefficient.

and BMI conditions, respectively. The reduction reflected the fact that although BMI increased the AM ratio in most cells, the decrease in STI was disproportionately greater so that the STI-predicted modulation more closely approximated that observed during BMI. Figure 11B plots the percent change in n_{CG} versus DI for these cells. Although both measures were reduced by BMI in most cells, the changes were not correlated. We note that expressing change in n_{CG} in terms of percentage is not ideal, given its exponential nature. As alternatives, we analyzed change in terms of absolute reduction in n_{CG} and DI and by normalizing for concomitant changes in STI. Neither procedure improved the correlation. We conclude that although reducing GABA_A-mediated inhibition altered both S-T structure and the static nonlinearity, the structural change was the more sensitive predictor of the reduction in direction selectivity.

DISCUSSION

Numerous studies have shown that iontophoretic application of bicuculline reduces direction selectivity (Sato et al. 1995; Sillito 1975, 1977; Sillito et al. 1980; Tsumoto et al. 1979; Wollman and Palmer 1993), thus demonstrating an important role for intracortical inhibition in generating this perceptually important (Pasternak et al. 1985) response property. However, translating these results into an understanding of how the inhibition operates has proved to be more difficult. Our study

reveals that, at least for layer 4 simple cells, inhibition sculpts the spatiotemporal structure of the receptive field, accentuating S-T orientation so as to produce greater directional tuning. In terms of the linear-static nonlinear exponent model, inhibition appears to operate primarily at the linear stage of spatiotemporal summation.

Here we discuss the results in light of the spatiotemporal model. We then consider the heterogeneity in the effect of BMI on direction selectivity and S-T structure, and its implications for excitatory mechanisms. Finally, we illustrate a connective scheme that accounts for our observations. We focus on layer 4 because BMI effects there can be interpreted in the context of the exponent model, although we briefly consider the layer 6 results.

Understanding BMI effects in the context of the LN model

Two aspects of our results clearly show that inhibition contributes to direction selectivity by altering S-T structure. First, BMI-induced reductions in selectivity nearly always were accompanied by reductions in S-T orientation, and changes in the two parameters were well correlated. Second, conventional linear predictions, based on response timing and amplitude, accounted well for absolute changes in the amplitude and phase (Fig. 10) of responses to drifting gratings. The success of these predictions confirms other evidence (Albrecht and Geisler 1991; DeAngelis et al. 1993a,b; Humphrey and Saul 1998; Jagadeesh et al. 1997; McLean et al. 1994; Reid et al. 1991) for linear spatiotemporal summation as a critical mechanism of directional tuning in simple cells. Also, it extends those population studies by showing how S-T structure and direction selectivity covary in single cells.

Although changes in structure account for much of the reduction in DI, the STI and conventional linear predictions underestimate directional tuning in control and BMI conditions (Fig. 9, *C* and *D*). This is expected because, in both conditions, nonlinearities exist that amplify directional biases produced by linear spatiotemporal summation. Although this helps to explain discrepancies between predicted and observed DI, we still must ask why the absolute changes in amplitude to drifting gratings were well predicted by the linear model (Fig. 10, *A* and *B*) given the static nonlinearity. The answer may lie in the fact that, for most cells, BMI reduced n_{CG} , our measure of the nonlinearity. Thus any change in amplitude to drifting gratings should have been well predicted by the linear model. In contrast to amplitude, the excellent predictions of response phase changes to drifting gratings are expected because response phase is not influenced by static nonlinearities.

Interpreting the weaker static nonlinearity (n_{CG}) during BMI application requires knowing what the nonlinearity reflects biologically. We have modeled it as an exponent but it may reflect a spike threshold or threshold plus amplification. In practice, exponents and thresholds produce similar effects: the accentuation of differences in cell discharge rates to optimal versus nonoptimal stimuli (Albrecht and Geisler 1991; Tolhurst and Heeger 1997). Carandini and Ferster (1998) recently provided support for threshold and amplification as processes underlying the static nonlinearity in simple cells. They measured the modulation of membrane potentials and discharge rates to drifting gratings. Directional tuning of the spikes was always greater than that of the potentials (Jagadeesh et al.

1997). The firing rates could be accounted for by applying a simple threshold to the membrane potentials followed by a linear gain.

These results suggest that the reduction in n_{CG} may be linked to changes in membrane potential relative to spike threshold. Given that inhibition acts to keep a cell's membrane potential below threshold (Berman et al. 1992; Ferster and Jagadeesh 1992), reducing inhibition by BMI should increase the proportion of time the potential rises above threshold. This will lead to increased firing rates in the preferred and nonpreferred directions, a change that we observed in most cells (Fig. 10). However, because the increase in the nonpreferred direction is proportionately greater, due to its smaller control response, direction selectivity will decrease. The BMI-induced reduction in n_{CG} thus may reflect an increase in membrane potential relative to spike threshold.

Whereas the reductions in n_{CG} help to account for heightened amplitudes and decreased direction selectivity, the reductions were not correlated with changes in DI, unlike the changes in S-T orientation. This indicates that inhibition affects direction selectivity primarily by accentuating S-T orientation. Inhibition secondarily affects the static nonlinearity, probably by lowering membrane potentials relative to spike threshold so as to suppress responses in the nonpreferred direction (Movshon et al. 1978). An additional possibility, which our data cannot address, is that inhibition also alters the gain of feedforward and recurrent excitation (Suarez et al. 1995).

The ability to dissociate the influence of BMI on linear versus static nonlinear mechanisms rests on the assumption that the nonlinearity does not affect response phase and hence does not alter S-T orientation. This assumption is reasonable given our measure of timing: fundamental response phase. For example, membrane potential fluctuations in response to sine-wave gratings are not always sinusoidal (cf. Figs. 7 and 8 in Jagadeesh et al. 1997). For a waveform that deviates from a sinusoid, simple DC shifts in the waveform relative to spike threshold might alter the resulting discharge profile and the timing of some spikes. However, the phase of the fundamental response would be affected little, as would be the S-T orientation. Only temporal shifts of the whole profile would significantly alter fundamental phase. Additionally, if a static nonlinearity did affect response phase and S-T orientation, then BMI-induced reductions in STI should correlate with the reductions in n_{CG} , but they did not ($r_s = -0.12$). Thus it is unlikely that changes in the static nonlinearity contributed to the reductions in S-T orientation. Those reductions likely reflect changes in spatiotemporal interactions among cells' inputs.

Heterogeneity in the effect of BMI on direction selectivity

The action of BMI on direction selectivity varied widely among cells, from small reductions to complete loss. These results conflict with those of Sillito et al. (1980), who reported that BMI eliminated direction selectivity in all simple cells studied. However, our results are in general agreement with those of Tsumoto et al. (1979), Wollman and Palmer (1993), and Sato et al. (1995), who also reported a wide range of BMI effects on direction selectivity. Numerous observations indicate that the heterogeneity here was not due to methodological

problems. First, potential variations between electrodes in reliably ejecting BMI partly were controlled for by performing titrations to assess the drug's ability to antagonize exogenously applied GABA. Second, differential effects of BMI were observed even in single penetrations. For example, in one track four cells were tested; BMI minimally affected direction selectivity in the first cell but virtually eliminated it in the last cell. Third, BMI significantly increased the visually evoked firing rates of nearly all cells relatively independent of the effect on direction selectivity, indicating that it effectively reduced some level of inhibition. Fourth, the strengths of BMI ejection currents were often less (~ 30 vs. >50 nA) for cells the direction selectivity of which was abolished than for cells showing little effect. Fifth, for a number of cells, after collecting the main set of data we continued to iontophorese BMI for up to 60 min and raised the current intensity as high as 200 nA to achieve maximal block. This nearly always resulted in oscillatory, bursty discharges unlinked to the visual stimulus followed by a silencing of activity. At no time did these prolonged ejections produce any reduction in directional tuning beyond that observed at lower currents. Sixth, most inhibitory synapses are located on or near the soma (Somogyi 1989) and the concentrations of BMI used should have effectively blocked their action. This is particularly the case in layer 4, where most cells are relatively small and compact (Martin and Whitteridge 1984). Taken together, these results indicate that genuine differences exist among cells in the contribution of GABA_A-mediated inhibition to direction selectivity and, likewise, to S-T structure.

We did not attempt to manipulate GABA_B-mediated inhibition. However, Baumfalk and Albus (1988) reported that iontophoresis of phaclophen, a GABA_B antagonist, rarely altered direction selectivity. In addition, intracellular blockade of both chloride (GABA_A) and potassium (GABA_B) channels causes a reduction but not an elimination of direction selectivity (Nelson et al. 1994). These, and the results given here, indicate that the directional tuning and S-T orientation remaining after blockade of inhibition reflects excitatory inputs onto simple cells.

Sources of inhibitory and excitatory inputs to direction selective cells

Here we consider the nature and sources of inputs to direction-selective cells in layer 4. The inhibitory inputs are clearly cortical in origin and most likely arise from other simple cells with receptive fields that are spatially and temporally offset from their targets (Maex and Orban 1996; Pollen and Ronner 1981). This conclusion is supported by the observation that reducing inhibition changed the temporal structure of layer 4 receptive fields. Complex cells lack spatiotemporally modulated responses, which are necessary to produce this effect.

Excitatory inputs to cortical cells arise from the LGN and cortex. We previously showed (Saul and Humphrey 1990) that lagged and nonlagged LGN cells (Mastrorade 1987) convey to cortex the range of timings needed to construct S-T oriented receptive fields. The unique timing signatures of the two afferent groups are observed readily in simple-cell receptive fields and can account for the progression of timings across these fields (Saul and Humphrey 1992a). Also direction selectivity in many simple cells varies with temporal frequency in a

manner predicted by the changing phase relationships between lagged and nonlagged cells as a function of temporal frequency (Saul and Humphrey 1992b). Further, Ferster et al. (1996) reported that cortical cooling, designed to suppress intracortical interactions, did not reduce directional tuning in layer 4 cells, as measured from membrane potentials in response to drifting gratings. These studies thus indicate that geniculocortical inputs play an important excitatory role in constructing direction-selective receptive fields.

The geniculate inputs likely contribute to S-T structure and directional tuning in layer 4 both by their direct connections to simple cells (Bullier and Henry 1979; Ferster and Lindstrom 1983; Martin and Whitteridge 1984) and by indirect connections via other cortical cells, some of which are inhibitory. In this regard our results and those of others (Sillito 1984) appear to conflict with the conclusion of Ferster et al. (1996) that, at least at the membrane potential level, inhibition is not necessary to produce directional tuning. However, the discrepancy may be less than it appears. The average DI in our layer 4 cells during BMI ejection was ~ 0.4 . This is on the high end of the DIs measured from membrane potential fluctuations (Jagadeesh et al. 1997). Perhaps the residual selectivity in our cells reflects geniculate-based directional biases of the membrane potentials. We would expect our DIs to be higher than those observed intracellularly because spike thresholds still affect the BMI data, accentuating directional biases. Nevertheless, we also found that inhibition accentuates S-T orientation and simple changes in spike threshold do not account for this. Therefore we predict that the removal of inhibition by cortical cooling should produce changes in S-T orientation that are observable at the membrane potential level. Unfortunately, no data on S-T structure during cooling exist to test this prediction. It remains to be determined whether the BMI and cooling results are compatible with a common interpretation.

Figure 12 provides a simple illustration, compatible with the present and previous (Saul and Humphrey 1990, 1992a) findings, of how an S-T well-oriented receptive field may be produced by inputs from other simple cells having certain spatiotemporal relationships. Simulated responses to a counterphasing grating are shown for an excitatory (A) and inhibitory (B) simple cell and their target (C). Only the first half of the grating spatial cycle is illustrated. Although not shown, responses in Fig. 12A are produced by rectified inputs from two LGN-like units—lagged and nonlagged—having relative spatial and temporal offsets of 0.1 and 0.15 cycles, respectively. Profiles in Fig. 12B reflect two other LGN inputs with similar relative offsets. The cortical receptive fields that result are each slightly S-T oriented (STIs = 0.23) and share the same preferred direction of motion. Linear summation of these two units (C) produces a receptive field with greater S-T orientation (STI = 0.64) and hence stronger directional tuning. An arc-tangent fit to the response phase versus spatial phase data is shown in Fig. 12D (●). Removing the inhibitory input to cell C would expose the excitatory structure, resulting in systematic shifts in the cell's response phase and a reduction in S-T orientation (○), similar to that observed experimentally (e.g., Fig. 5C). Note that receptive fields receiving direct LGN input may be more or less S-T oriented than shown here, depending on the range of response timings among the inputs.

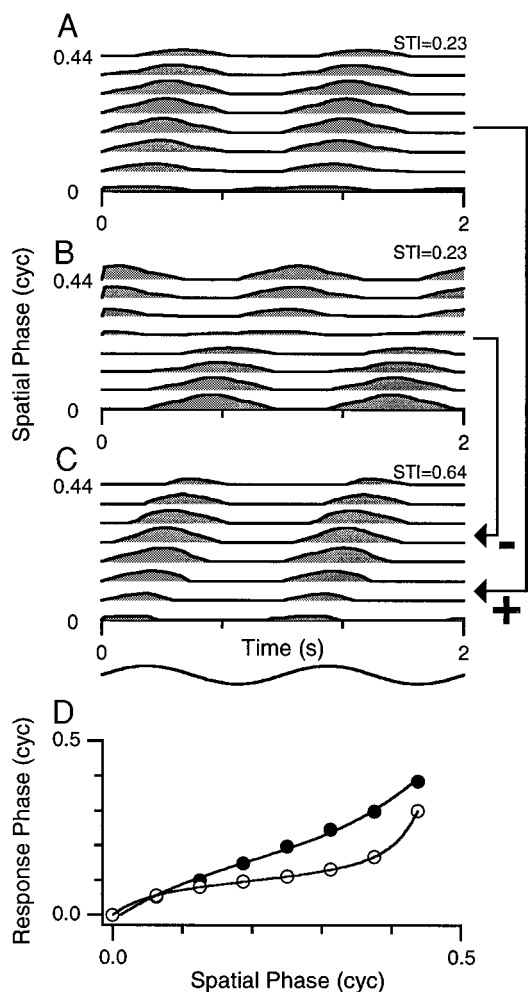


FIG. 12. Illustration of a connective scheme that would produce a highly S-T-oriented receptive field. Simulated responses of an excitatory (A) and inhibitory (B) simple cell and their target (C) to a counterphase grating at 8 spatial phases covering one-half of the grating cycle. Responses in A reflect the rectified output of 2 ON center, LGN-like units (not illustrated) the spatial phases of which, relative to 0 phase of the grating, are 0.0 and 0.1 cycles, respectively, and the temporal phases of which are 0.05 and 0.20 cycles, respectively. B: spatial and temporal phases of 2 other ON center inputs are 0.25 and 0.25 cycles, respectively, for 1 input and 0.35 and 0.05 cycles for the other. Spatiotemporal offsets of the afferents produce slight S-T orientation in the recipient receptive fields. Linear summation of the rectified outputs of the 2 cortical cells produces a third receptive field (C) with greater S-T orientation. STI values are indicated for each receptive field. D: arctangent fit to the phase data in A (○) and C (●), to illustrate how removal of inhibition would change timing and reduce S-T orientation in cell C.

This illustration does not address obvious complexities such as spatially opponent inhibition, excitatory and inhibitory feedback at all of the illustrated stages, and the large numbers of neurons that must interact. These and other spatiotemporal interactions have been modeled by others (Maex and Orban 1996; Suarez et al. 1995). Maex and Orban (1996) have shown that the S-T interactions can account for many stimulus-dependent behaviors of direction-selective cells. Here we illustrate excitation and inhibition as sharing the same preferred direction, but in principle cross- and nondirectional inhibition could interact with excitatory inputs to produce S-T-oriented structure. A key difference between our model (Saul and Humphrey 1992a) and that of Maex and Orban (1996), however, is the source

of the timings that produce S-T orientation. Clearly, in the cat, the necessary range of timing delays is present in the LGN relay cells (Saul and Humphrey 1990). Their existence precludes the need to create timing delays in cortex using polysynaptic circuits, *N*-methyl-D-aspartate receptors (Maex and Orban 1996) and/or GABA_B receptors (Suarez et al. 1995).

Directional mechanisms in layer 6

Unlike layer 4, direction-selective cells in layer 6 display weak first-order S-T orientation, and even the addition of static nonlinearities does not account for their directional tuning (Murthy et al. 1998). Similarly, BMI had no consistent effect on the cells' first-order S-T structure despite reducing direction selectivity. These results indicate that dynamic nonlinear interactions predominate in layer 6. Such interactions are detectable using two bars flashed sequentially across the receptive field (Emerson and Citron 1992). The second-order S-T oriented structures revealed by this indicate that directional tuning reflects nonlinear facilitatory and suppressive interactions in the preferred and nonpreferred directions. An obvious prediction is that BMI should lessen the suppression and reduce second-order S-T orientation.

We thank P. Baker for computer programming, M. Kieler for electronics support, and J. Feidler and A. Saul for helpful discussions. We are particularly grateful to Dr. Kaiqi Sun for instructing us in the manufacture and use of the iontophoresis arrays and for participating in the early experiments.

This research was supported by National Eye Institute Grant EY-06459 and a Core Grant for Vision Research (EY-08098) to the Eye and Ear Institute of Pittsburgh.

Present address of A. Murthy: Dept. of Psychology, 301 Wilson Hall, Vanderbilt University, Nashville, TN 37240.

Address for reprint requests: A. L. Humphrey, Dept. of Neurobiology, University of Pittsburgh, School of Medicine, E1440 Biomedical Science Tower, Pittsburgh, PA 15261.

Received 1 July 1998; accepted in final form 24 November 1998.

REFERENCES

- ALBRECHT, D. G. AND GEISLER, W. S. Motion selectivity and the contrast-response function of simple cells in the visual cortex. *Vis. Neurosci.* 7: 531–546, 1991.
- BAUMFALK, U. AND ALBUS, K. Phaclofen antagonizes baclofen-induced suppression of visually evoked responses in the cat's striate cortex. *Brain Res.* 463: 398–402, 1988.
- BERMAN, N. J., DOUGLAS, R. J. AND MARTIN, K.A.C. GABA-mediated inhibition in the neural networks of visual cortex. In: *Progress in Brain Research. GABA in the Retina and Central Nervous System*, edited by R. R. Mize, R. E. Marc, and A. M. Sillito. New York: Elsevier, 1992, vol. 90, p. 443–476.
- BULLIER, J. AND HENRY, G. H. Laminar distribution of first-order neurons and afferent terminals in cat striate cortex. *J. Neurophysiol.* 42: 1271–1281, 1979.
- CARANDINI, M. AND FERSTER, D. The iceberg effect and orientation tuning in cat V1. *Invest. Ophthalmol. Vis. Sci.* 39: S239, 1998.
- DEANGELIS, G. C., OHZAWA, I., AND FREEMAN, R. D. Spatiotemporal organization of simple-cell receptive fields in the cat's striate cortex. I. General characteristics and postnatal development. *J. Neurophysiol.* 69: 1091–1117, 1993a.
- DEANGELIS, G. C., OHZAWA, I., AND FREEMAN, R. D. Spatiotemporal organization of simple-cell receptive fields in the cat's striate cortex. II. Linearity of temporal and spatial summation. *J. Neurophysiol.* 69: 1118–1135, 1993b.
- EMERSON, R. C. AND CITRON, M. C. Linear and nonlinear mechanisms of motion selectivity in simple cells of the cat's striate cortex. In: *Non-linear Vision Determinants of Neural Receptive Fields, Function and Net-*

- works, edited by R. B. Pinter and B. Nabet. Boca Raton: CRC, 1992, p. 75–89.
- FERSTER, D., CHUNG, S., AND WHEAT, H. Orientation selectivity of thalamic input to simple cells of cat visual cortex. *Nature* 380: 249–252, 1996.
- FERSTER, D. AND JAGADEESH, B. EPSP-IPSP interactions in cat visual cortex studied with in vivo whole-cell patch recording. *J. Neurosci.* 12: 1262–1274, 1992.
- FERSTER, D. AND LINDSTROM, S. An intracellular analysis of geniculocortical connectivity in area 17 of the cat. *J. Physiol. (Lond.)* 342: 181–215, 1983.
- HAVEY, D. C. AND CASPARI, D. M. A simple technique for constructing “piggy-back” multibarrel microelectrodes. *Electroencephalogr. Clin. Neurophysiol.* 48: 249–251, 1980.
- HEEGER, D. J. Modeling simple-cell direction selectivity with normalized, half-squared, linear operators. *J. Neurophysiol.* 70: 1885–1898, 1993.
- HUBEL, D. H. AND WIESEL, T. N. Receptive fields, binocular interaction and functional architecture in the cat’s visual cortex. *J. Physiol. (Lond.)* 160: 106–154, 1962.
- HUMPHREY, A. L. AND SAUL, A. B. Strobe rearing reduces direction selectivity in area 17 by altering spatiotemporal receptive-field structure. *J. Neurophysiol.* 80: 2991–3004, 1998.
- HUMPHREY, A. L., SUR, M., UHLRICH, D. J., AND SHERMAN, S. M. Projection patterns of individual X- and Y-cell axons from the lateral geniculate nucleus to cortical area 17 in the cat. *J. Comp. Neurol.* 233: 159–189, 1985.
- JAGADEESH, B., WHEAT, H. S., KONTSEVICH, L. L., TYLER, C. W., AND FERSTER, D. Direction selectivity of synaptic potentials in simple cells of cat visual cortex. *J. Neurophysiol.* 78: 2772–2789, 1997.
- MAEX, R. AND ORBAN, G. A. Model circuit of spiking neurons generating directional selectivity in simple cells. *J. Neurophysiol.* 75: 1515–1545, 1996.
- MARTIN, K.A.C. AND WHITTERIDGE, D. Form, function, and intracortical projections of spiny neurons in the striate cortex of the cat. *J. Physiol. (Lond.)* 353: 463–504, 1984.
- MASTRONARDE, D. N. Two classes of single-input X-cells in cat lateral geniculate nucleus. I. Receptive-field properties and classification of cells. *J. Neurophysiol.* 57: 381–413, 1987.
- MCLEAN, J. AND PALMER, L. A. Contribution of linear spatiotemporal receptive field structure to velocity selectivity of simple cells in area 17 of cat. *Vision Res.* 29: 675–679, 1989.
- MCLEAN, J., RAAB, S., AND PALMER, L. A. Contribution of linear mechanisms to the specification of local motion by simple cells in areas 17 and 18 of the cat. *Vis. Neurosci.* 11: 271–294, 1994.
- MILLER, I. AND FREUND, J. E. *Probability and Statistics for Engineers*. New Delhi: Prentice-Hall, 1985.
- MOVSHON, J. A., THOMPSON, I. D., AND TOLHURST, D. J. Spatial summation in the receptive fields of simple cells in the cat’s striate cortex. *J. Physiol. (Lond.)* 283: 53–77, 1978.
- MURTHY, A. N., HUMPHREY, A. L., SAUL, A. B., AND FEIDLER, J. C. Laminar differences in the spatiotemporal structure of simple cell receptive fields in cat area 17. *Vis. Neurosci.* 15: 239–256, 1998.
- NELSON, S., TOTH, L., SHETH, B., AND SUR, M. Orientation selectivity of cortical neurons during intracellular blockade of inhibition. *Science* 265: 774–777, 1994.
- O’LEARY, J. L. Structure of the area striata of the cat. *J. Comp. Neurol.* 75: 131–164, 1941.
- PASTERNAK, T., SCHUMER, R. A., GIZZI, M. S., AND MOVSHON, J. A. Abolition of visual cortical direction selectivity affects visual behavior in cats. *Exp. Brain Res.* 61: 214–217, 1985.
- POLLEN, D. A. AND RONNER S. F. Phase relationships between adjacent simple cells in the visual cortex. *Science* 212: 1409–1411, 1981.
- REID, R. C., SOODAK, R. E., AND SHAPLEY, R. M. Directional selectivity and spatiotemporal structure of receptive fields of simple cells in cat striate cortex. *J. Neurophysiol.* 66: 505–529, 1991.
- SATO, H., KATSUYAMA, N., TAMURA, H., HATA, Y., AND TSUMOTO, T. Mechanisms underlying direction selectivity of neurons in the primary visual cortex of the macaque. *J. Neurophysiol.* 74: 1382–1394, 1995.
- SAUL, A. B. AND HUMPHREY, A. L. Spatial and temporal response properties of lagged and nonlagged cells in the cat lateral geniculate nucleus. *J. Neurophysiol.* 64: 206–224, 1990.
- SAUL, A. B. AND HUMPHREY, A. L. Evidence of input from lagged cells in the lateral geniculate nucleus to simple cells in cortical area 17 of the cat. *J. Neurophysiol.* 68: 1190–1207, 1992a.
- SAUL, A. B. AND HUMPHREY, A. L. Temporal frequency tuning of direction selectivity in cat visual cortex. *Vis. Neurosci.* 8: 365–372, 1992b.
- SILLITO, A. M. The contribution of inhibitory mechanisms to the receptive field properties of neurons in the striate cortex of the cat. *J. Physiol. (Lond.)* 250: 305–329, 1975.
- SILLITO, A. M. Inhibitory processes underlying the directional specificity of simple, complex, and hypercomplex cells in the cat’s visual cortex. *J. Physiol. (Lond.)* 271: 775–785, 1977.
- SILLITO, A. M. Functional considerations of the operation of GABAergic inhibitory processes in the visual cortex. In: *Cerebral Cortex*, edited by E. G. Jones and A. Peters. New York: Plenum Press, 1984, vol. 2, p. 91–117.
- SILLITO, A. M., KEMP, J. A., MILSON, J. A., AND BERARDI, N. A re-evaluation of the mechanisms underlying simple cell orientation selectivity. *Brain Res.* 194: 517–520, 1980.
- SKOTTUN, B. C., DEVALOIS, R. L., GROSOF, D. H., MOVSHON, J. A., ALBRECHT, D. G., AND BONDS, A. B. Classifying simple and complex cells on the basis of response modulation. *Vision Res.* 31: 1079–1086, 1991.
- SOMOGYI, P. Synaptic organization of GABAergic neurons and GABA_A receptors in the lateral geniculate nucleus and visual cortex. In: *Neural Mechanisms of Visual Perception*, edited by D.M.K. Lam and C. D. Gilbert. Houston: Gulf, 1989, p. 35–62.
- SUAREZ, H., KOCH, C., AND DOUGLAS, R. Modeling direction selectivity of simple cells in striate visual cortex within the framework of the canonical microcircuit. *J. Neurosci.* 15: 6700–6719, 1995.
- TOLHURST, D. J. AND HEEGER, D. J. Comparison of contrast-normalization and threshold models of responses of simple cells in cat striate cortex. *Vis. Neurosci.* 14: 293–309, 1997.
- TSUMOTO, T., ECKART, W. AND CREUTZFELDT, O. D. Modification of orientation sensitivity of cat visual cortex neurons by removal of GABA-mediated inhibition. *Exp. Brain Res.* 34: 351–363, 1979.
- WOLLMAN, D. E. AND PALMER, L. A. The effects of GABA blockade on the spatiotemporal receptive field structure of neurons in cat striate cortex. *Invest. Ophthalm. Vis. Sci.* 34: S908, 1993.